



Cellular uptake of magnetite nanoparticles enhanced by NdFeB magnets in staggered arrangement



Yi-Ching Lu^a, Fan-Yu Chang^a, Shu-Ju Tu^b, Jyh-Ping Chen^c, Yunn-Hwa Ma^{a,d,*}

^a Department of Physiology and Pharmacology & Healthy Aging Research Center, Guishan, Taoyuan City 33302, Taiwan, ROC

^b Department of Medical Imaging and Radiological Sciences, Chang Gung University, Guishan, Taoyuan City 33302, Taiwan, ROC

^c Department of Chemical and Materials Engineering, Chang Gung University, Guishan, Taoyuan City 33302, Taiwan, ROC

^d Department of Neurology, Chang Gung Memorial Hospital, Guishan, Taoyuan City 33305, Taiwan, ROC

ARTICLE INFO

Keywords:

Magnetic nanoparticles
Cellular uptake
Magnet
Culture
Homogeneity

ABSTRACT

Magnetic force may greatly enhance uptake of magnetic nanoparticles (MNPs) by cultured cells; however, the effects of non-uniformity of magnetic field/ magnetic gradient on MNP internalization in culture has not been elucidated. Cellular uptake of polyacrylic acid coated-MNP by LN229 cells was measured with cylindrical NdFeB magnets arranged in a staggered pattern. The magnetic field generated by placing a magnet underneath (H-field) elicited a homogenous distribution of MNPs on the cells in culture; whereas the field without magnet underneath (L-field) resulted in MNP distribution along the edge of the wells. Cell-associated MNP (MNP_{cell}) appeared to be magnetic field- and concentration-dependent. In H-field, MNP_{cell} reached plateau within one hour of exposure to MNP with only one-min application of the magnetic force in the beginning of incubation; continuous presence of the magnet for 2 h did not further increase MNP_{cell}, suggesting that magnetic force-induced uptake may be primarily contributed to enhanced MNP sedimentation. Although MNP distribution was much inhomogeneous in L-field, averaged MNP_{cell} in the L-field may reach as high as 80% of that in H-field during 1–6 h incubation, suggesting high capacity of MNP internalization. In addition, no significant difference was observed in MNP_{cell} analyzed by flow cytometry with the application of H-field of staggered plate *vs.* filled magnet plate. Therefore, biological variation may dominate MNP internalization even under relatively uniformed magnetic field; whereas non-uniformed magnetic field may serve as a model for tumor targeting with MNPs *in vivo*.

1. Introduction

Magnetic nanoparticles (MNPs) with iron oxide core and polymer coating have been extensively studied and demonstrated with many advantages including easy synthesis, inoffensive toxicity [1], and reactive surface that can be readily modified with excellent biocompatibility [2–4]. There has been spanning a wide range of MNPs in bio-applications that include drug delivery [2–5], gene transfection [6–10], hyperthermia [4,5,11,12], magnetic separation [5], as contrast media in magnetic resonance imaging [2,12–14], and as sensors for metabolites and other biomolecules [12]. In these applications, the magnetic properties of MNPs are crucial, which exert a rapid magnetization in response to an external magnetic field, and lose the magnetic responsiveness while removal of the magnetic field, known as superparamagnetism [15]. When cultured cells are exposed to MNP under the influence of an applied magnetic field, the superparamagnetism of MNPs allows enhancement of MNP sedimentation and enhanced

cellular internalization [16,17]. It is assumed that an enhanced sedimentation may mediate the effects of enhanced internalization.

A variety of cultured cells have been demonstrated to uptake MNPs, including primary [18] cells and many tumor cells [18–21]. Cellular internalization of nanoparticles is primarily *via* endocytosis pathways [15,22]. Several parameters including size, shape, and surface characteristics of nanoparticles may determine the endocytotic mechanisms involved [15,22]. Based on the size of the uptaken cargos, endocytosis may be divided into two categories, phagocytosis and pinocytosis [22,23]. Uptake of particles with nanometer size range may be mediated by pinocytosis involving different molecules including clathrin or caveolae [22]. Surface characteristics of nanoparticles, such as charge, critically affect how nanoparticles interact with proteins and cells in culture and in circulation [22–24]. Therefore, cellular uptake of nanoparticles may be influenced by different surface coating with polymers [22]. For instance, coating the nanoparticles with polyethylene glycol (PEG) may attenuate protein adsorption and consequently,

* Corresponding author at: Department of Physiology and Pharmacology, Chang Gung University, 259 Wen-Hua 1st Road, Kwei-Shan, Tao-Yuan 333, Taiwan, ROC.
E-mail address: yhma@mail.cgu.edu.tw (Y.-H. Ma).

reduce cellular uptake of nanoparticles [24–26].

It has been demonstrated that magnetic flux density may affect MNP internalized in culture [18,21,26–28] by augmenting interaction among MNPs, and enhancing interaction with plasma membrane. Magnetic field aligns the magnetic moment of MNPs and creates attractive dipole–dipole interaction between MNPs, leading to MNP aggregation [27] and attracting MNPs toward the surface of the magnet [29]. Application of magnetic force in culture has been conducted by placement of permanent magnet underneath the culture plate [10,16,19,21,26,29], which creates a force on MNP clusters, draws MNPs in contact with the cell surface, and thus increases MNP internalization [16,18,28]. Such effects of magnetic force on MNP internalization may be applied in gene transfection [5,7–10] or targeted drug delivery [3–5,12]. However, it is not clear whether magnetic force may further enhance MNP uptake in addition to enhance sedimentation.

Cultured cells may be exposed to magnetic field that are generated by an array of permanent magnets, which are commercially available [16] or home-made with NdFeB magnets [10,19,21,26]. Previous studies have demonstrated using rectangular block of NdFeB magnet under 6- or 24-well plate [10] or cylindrical magnets in 96-well plate [6,10], which significantly increase the transfection efficiency by 2 to thousands fold [10]. However, the magnetic flux density and magnetic gradient of the individual magnet may be influenced by adjacent magnets in a compact arrangement under a culture plate with multiple wells, resulting in relatively non-uniformed magnetic field gradients [29], which may result in inhomogeneous distribution of MNPs and subsequently, high variation of MNP internalization in cell population of each well [10], and thus hinder further analysis of individual cells by techniques such as flow cytometry. Alternatively, cells may be seeded in every second well to avoid such problem [21]. Previous simulation suggested non-uniformity of the magnetic field generated by the magnet array with alternating magnetization [29]. However, it is not known whether magnet array with staggered arrangement may produce a relatively uniformed magnetic field to avoid potentially heterogeneous distribution of MNPs in culture.

We thus characterized MNP uptake by tumor cells under a relatively high magnetic field generated by a staggered arrangement of the NdFeB magnets and ask whether continuous presence of magnetic force may enhance uptake in addition to enhance sedimentation, and whether the cells in the wells without a magnet underneath may respond to the magnets underneath adjacent wells. In this study, internalization of MNP with polyacrylic acid (PAA) coating was determined, which has been demonstrated to serve as an effective carrier system in magnetic targeting with good stability and bioavailability [30,31]. Such anionic polymer has been used to stabilize MNP in water-based suspensions by providing electrostatic and steric repulsion against particle aggregation [31,32]. It has been demonstrated that PAA-coated MNP may be readily internalized *via* endocytosis within as short as 15 min [33] by different cells in culture [34,35]. Our results demonstrated that even under relatively high magnetic field provided by staggered arrangement of NdFeB magnets underneath, variation of MNP uptake may still occur, and that magnet-induced sedimentation may be the major mechanism in uptake enhancement by the NdFeB magnet placed underneath.

2. Materials and methods

2.1. Materials

Superparamagnetic nanoparticles with polyacrylic acid coating (fluidMAG-PAS; 200 nm) were purchased from Chemicell (Berlin, Germany). Fetal bovine serum (FBS) was purchased from PAA Laboratories GmbH (Pasching Austria). Trypsin-EDTA, Dulbecco's Modified Eagle Medium (DMEM) was purchased from Gibco BRL (Grand Island, NY). Penicillin/streptomycin/amphotericin B was pur-

chased from Upstate (Lake Placid, NY, USA). Hydrochloric acid (HCl), ammonium persulphate (APS), potassium thiocyanate (KSCN), 4-(2-hydroxyethyl)-1-piperazineethanesulfonic acid (HEPES), 3-(4,5-Dimethylthiazol-2-yl)-2,5-diphenyl-tetrazolium bromide (MTT) were purchased from Sigma (St. Louis, MO). Dimethyl sulfoxide was purchased from Bioman Scientific Co. (Fairfield, OH). The magnetic plates in staggered pattern (6 well plate: MTR-06, 24 well plate: MTR-24) were obtained from MagQu, Taiwan, ROC.

2.2. Cell culture

Human glioma cell line LN229 were obtained from American Type Culture Collection (Manassas, VA), and were cultured in DMEM supplemented with 10% FBS and 1% penicillin/streptomycin/amphotericin B mixture. The cells were maintained at 37 °C in an incubator supplied with 5% CO₂.

2.3. Application of magnetic force on cultured cells

The cells were cultured in every well of 6- or 24-well plates to 90% confluence for further study. The magnetic plate with cylindrical NdFeB magnet array in staggered arrangement (Fig. 1) was placed underneath the cell culture plate. Cells grown in the wells with the magnet placed underneath were subjected to relatively high and uniformed magnetic dragging force of ~4 kGauss with variation less than 10% (H magnetic field, Table 1). In contrast, cells grown in the wells with no magnet underneath were subjected to relatively low and non-uniformed magnetic force (L magnetic field, Table 1). In some experiments, a home-made magnetic plate with 24 pieces of cylindrical NdFeB magnet with a diameter of 1.8 cm arranged to provide a magnetic field of 3.4 kG at the center of each well was applied. The magnetic field intensity of magnets was measured by a hand-held Gauss meter (FW Bell 5180, Sypris Test and Measurement, FW Bell, FL) equipped with a transverse probe.

2.4. Dark field microscopy

Cells were cultured on round cover slips (22 mm diameter; Assistant, Glaswarenfabrik Karl Hecht, Germany) that was placed in the wells of 6-well plates prior to be exposed to MNP. Cells were then incubated with PAA-coated MNPs (80 µg/well) under magnetic field for 2 h, followed by washing with PBS, fixing with 4% paraformaldehyde and mounting on the slide glass for imaging. Images of cells with MNP uptake was captured with light scattering microscope Olympus IX71 equipped with CytoViva Adapter (CytoViva Advanced Darkfield Illumination System; Aetos Technologies, Inc., Auburn, AL).

2.5. MNP assay

The cells were cultured in every well of 6- or 24-well plates to 90% confluence. Cells were then incubated with MNPs for 1–6 h. The cells were digested with trypsin and the cell suspension was subjected to HCl (2.1% v/v) and incubated at 60 °C for 3 h. Ammonium persulphate (95 µg/ml) was then added to convert ferrous ion to ferric ion, followed by addition of potassium thiocyanate (87 mM), allowing formation of iron-thiocyanate complex. Iron content was determined at OD₄₉₀ with a microplate reader (Victor 3™ Multilabel Plate Reader, PerkinElmer, MA, USA). A calibration curve with serial dilution of known concentrations (w/v) of MNPs was prepared to analyze the amount of MNP uptake.

2.6. Flow cytometry analysis

In response to MNP uptake, cells were characterized with flow cytometry for determination of FSC (forward scatter) and SSC (side scatter), which correlates with the cell volume and the complexity of

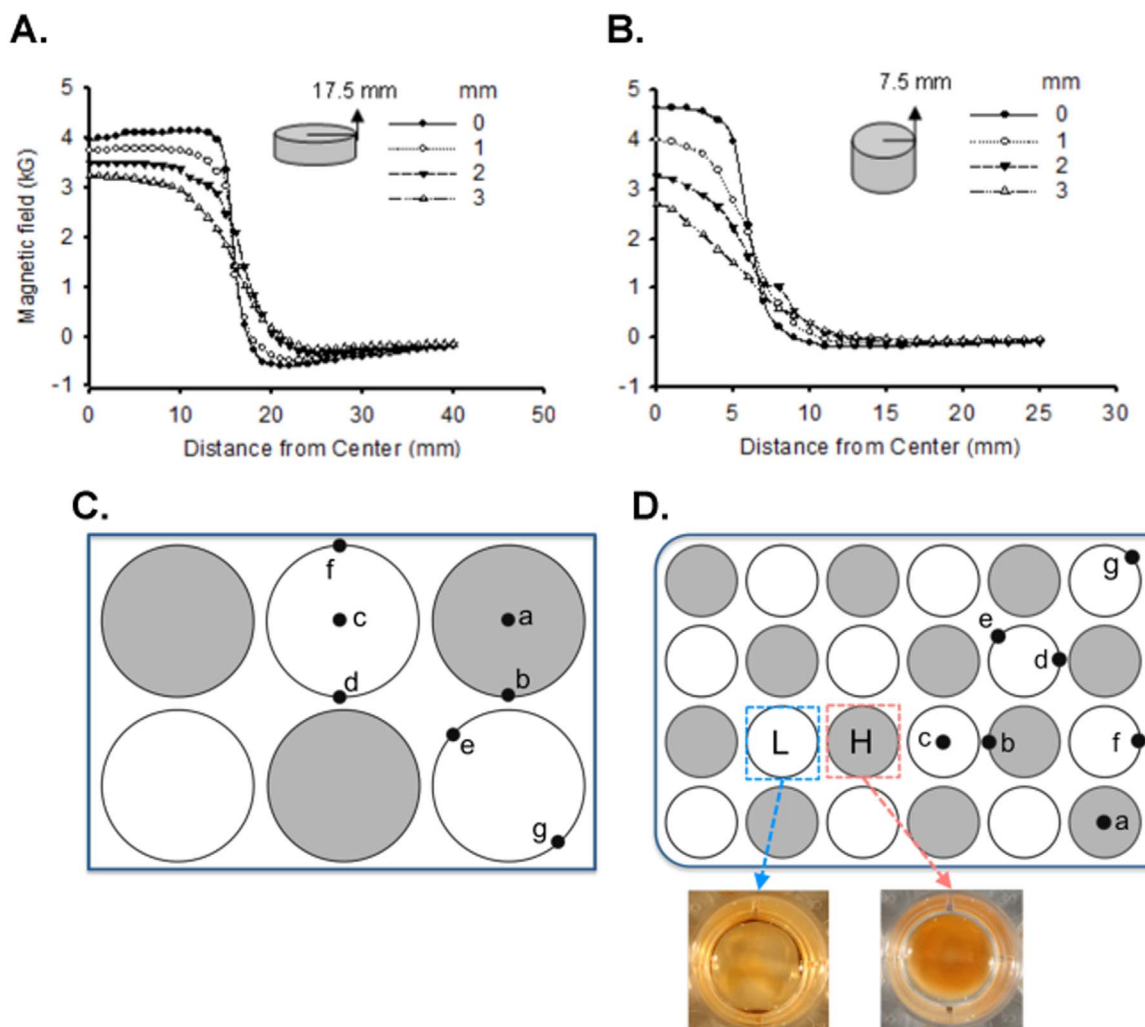


Fig. 1. Magnetic field designed for 6-well (A) and 24-well (B) culture plates. Cylindrical NdFeB magnets were placed in wells (shaded area) that exerted high and relative uniform magnetic field (H), whereas the wells without placement of the magnet were only subjected to adjacent magnets with lower and relative non-uniform magnetic field (L). Magnetic field was measured at each spotted sites (C & D) with a Gauss meter. The MNP distribution on single layer of cultured cells in medium without phenol red for observation of MNP distribution under the influence of H- & L-field for 10 min was demonstrated in photos (D).

Table 1

Magnetic field (kGauss) at specific sites (a-f) of 6- or 24-well plates as designated in Figs. 1C & D. The measurements were conducted with (H) or without (L) an NdFeB magnet underneath. Data are presented as mean ± SE; numbers of each measurement at different but equivalent spots in the same plate are indicated in parenthesis.

Magnetic field sites		6-well	24-well
H	a	4.0 ± 0.1 (3)	4.07 ± 0.21 (12)
	b	3.9 ± 0.1 (6)	3.81 ± 0.31 (10)
L	c	0.5 ± 0.2 (3)	0.35 ± 0.16 (8)
	d	1.0 ± 0.1 (7)	0.55 ± 0.21 (10)
	e	0.9 ± 0.04 (4)	0.67 ± 0.15 (7)
	f	0.41 (1)	0.26 ± 0.10 (8)
	g	0.17 (2)	0.019 (2)

cytosolic structure, respectively. Briefly, cells were cultured in 24-well plates and incubated with PAA-coated MNPs. After incubation for 2 h, cells were washed twice with ice-cold PBS prior to trypsinization for analysis. After centrifugation, the resulting cell pellet was resuspended in PBS, and subjected to analysis using flow cytometer (BD FACSCalibur™, NJ, USA). The FSC (forward scatter) and SSC (side scatter) distribution were gated based on normal cell conditions acquired from a control group without MNP. Side scatter (SSC) is

generally thought to be an indicative of the granularity/complexity of the cells while forward scatter (FSC) provides information on the overall size of cells.

2.7. MTT assay

After 2 h incubation with various MNP concentrations, the medium was removed and washed with PBS, followed by incubation with MTT (0.5 mg/ml) at 37 °C for 1 h. The dark blue formazan crystals generated by the mitochondrial dehydrogenase were dissolved with dimethyl sulfoxide followed by measurement of OD₅₄₀.

2.8. Statistical analysis

Values are expressed as mean ± SE. Effects of drugs were examined by Student *t*-test, 2-way analysis of variance (ANOVA) followed by Duncan's post hoc test when appropriate. Statistical significance was declared as a *p* value of < 0.05.

3. Results

Effects of magnetic field on cellular uptake of MNPs were observed by dark field microscopy. Fig. 2 illustrates representative results of MNP uptake in H-field in the 6-well plate for one min (m) vs. 2 h (M).

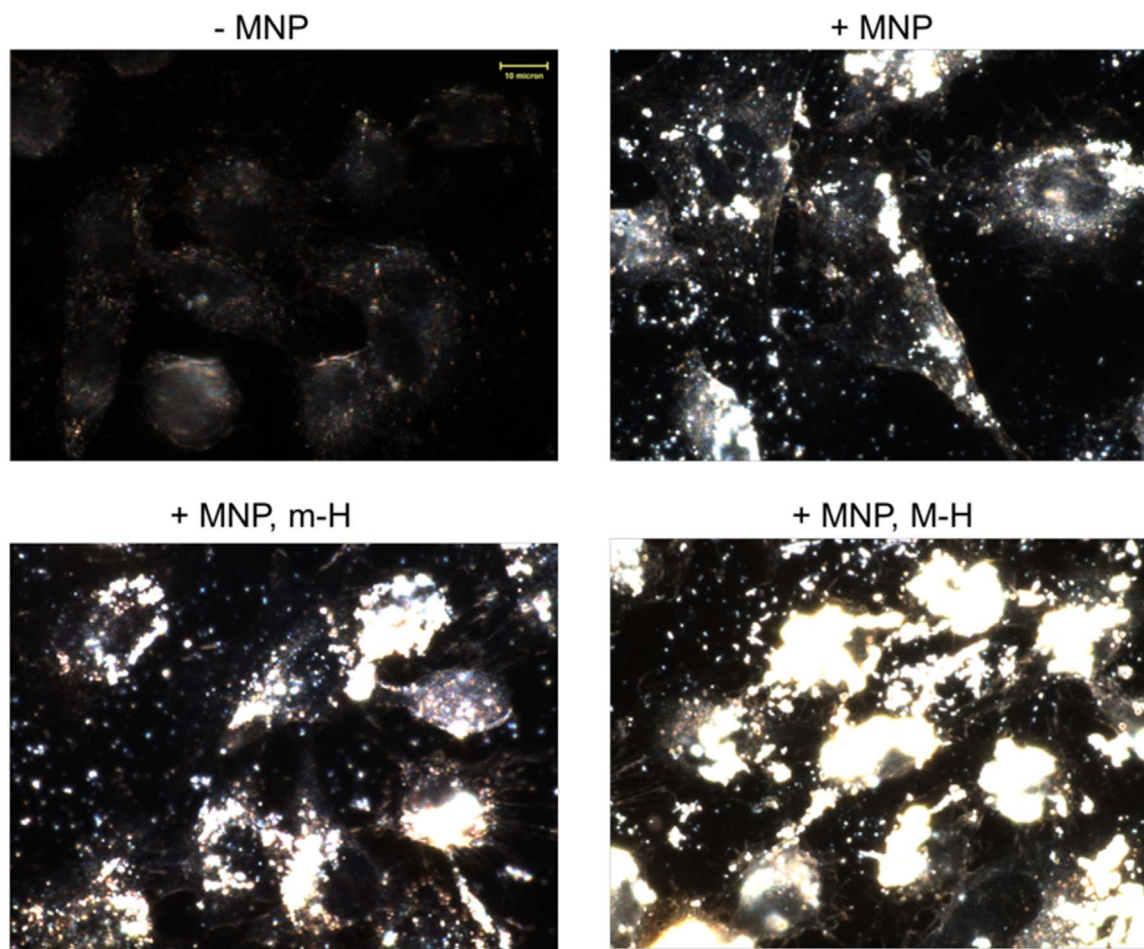


Fig. 2. Representative imaging of MNP uptake by LN229 cells in uniform magnetic field. Cells were exposed to MNP ($80 \mu\text{g}/\text{well}$; $8 \mu\text{g}/\text{cm}^2$) for 2 h with high (H) intensity of magnetic field for one min (m) or during the whole incubation time (M). The images were taken with dark field microscope at $\times 1000$ magnification.

With this system, one-min application of the magnet caused MNPs to settle at the bottom of the culture well and get in contact with the cells. Exposure to MNP in H-field for 1 min (m-H) or 2 h (m-H) during the 2-hr incubation greatly enhanced MNP signals, suggesting the application of the magnet may increase cell-associated MNP (MNP_{cell}).

Iron content of cultured cells was determined for assessment of MNP uptake, as illustrated in Fig. 3A. MNP_{cell} in L- vs. H-field were 1.3-fold vs. 3.1-fold of that with no magnetic field, respectively. Further study with flow cytometry demonstrated similar results, as SSC distribution curve of H-field shifted significantly to the right (Fig. 3B). The scattered plots of FSC vs. SSC (Fig. 3C-F) shifted upwards in the presence of MNP, suggesting that cellular uptake of MNP induced an increase in cellular complexity/granularity. Cells treated with MNP in H-field (Fig. 3F) exerted the highest SSC cells among all conditions, with the cells located in SSC region above 500, i.e., the right upper quartile, was about 2- and 2.8-fold of that in the corresponding areas of L-field (Fig. 4E) and without magnet (-mag; Fig. 4D), respectively ($p < 0.05$). In addition, a decrease in the FSC in magnetic field was observed corresponding to the increase in SSC, suggesting the size of the cells decreased after MNP uptake.

Fig. 4A illustrates time-associated effects of magnetic field on MNP uptake by LN229 cells, which were further depicted in pairs in Fig. 4B-E. In L-field, MNP_{cell} increased with time (m-L), and was approximately 2–2.3 fold of those exposed for only one min to the L-field (m-L) at corresponding time point (Fig. 4B). In H-field, MNP_{cell} achieved nearly maximal within one h of exposure to MNPs, suggesting the effects are primarily due to H-field-induced sedimentation (Fig. 4C-E). Nevertheless, MNP uptake in cells exposed to constant H-field for 4

and 6 h (m-H) was 1.4 and 1.6 times of that with transient H-field (m-H), respectively (Fig. 4C). In addition, cells incubated with MNPs for 1 and 6 h with one-min exposure to H-field (m-H) exerted 3.8 and 2.0 fold of MNP uptake of that to L-field (m-L; Fig. 4D), suggesting one-min exposure to L-field may not be enough to allow strong interaction of MNPs with cellular membrane in culture. When exposed to H- vs. L-magnetic force for 1–6 h, MNP uptake in cells exposed to constant H-field was 1.3–1.8 fold of that with L-field (Fig. 4E). Concentration-dependent effects on MNP_{cell} was also observed in Fig. 5, especially with H-field (Fig. 5C-E). The MNP uptake in our system may be up to $14 \text{ pg}/\text{cell}$ after incubation of $25 \mu\text{g}/\text{cm}^2$ MNPs for 2 h in the presence of H-field. The difference of MNP_{cell} in H- vs. L-magnetic field was similar with transient (Fig. 5D) vs. constant (Fig. 5E) exposure, suggesting available MNP for uptake is a dominant effect for amount of cellular uptake.

In response to MNP uptake under above mentioned conditions for 2 h, mitochondrial dehydrogenase activity, as evaluated with MTT assay, decreased to 70–88% of the control ($p < 0.05$, Fig. 6), which was not correlated with amount of MNP uptake under each condition in Fig. 5. In this experiment, H_2O_2 (57 mM) caused 93% reduction of the enzyme activity in LN229 cells (Data not shown).

To observe the cellular uptake of MNPs affected by magnetic field with different magnet arrangement, flow cytometry analysis was conducted. Fig. 7 illustrates MNP uptake by cells in H- and L-field of staggered plate and by cells subjected to filled and alternating arranged magnetic field from underneath and adjacent wells (M-F) in the 24-well plate for 2 h. The cell distribution of $\text{SSC} > 300$ is similar to that in H-field of staggered plate (M-H) and filled magnet plate (M-F), suggesting

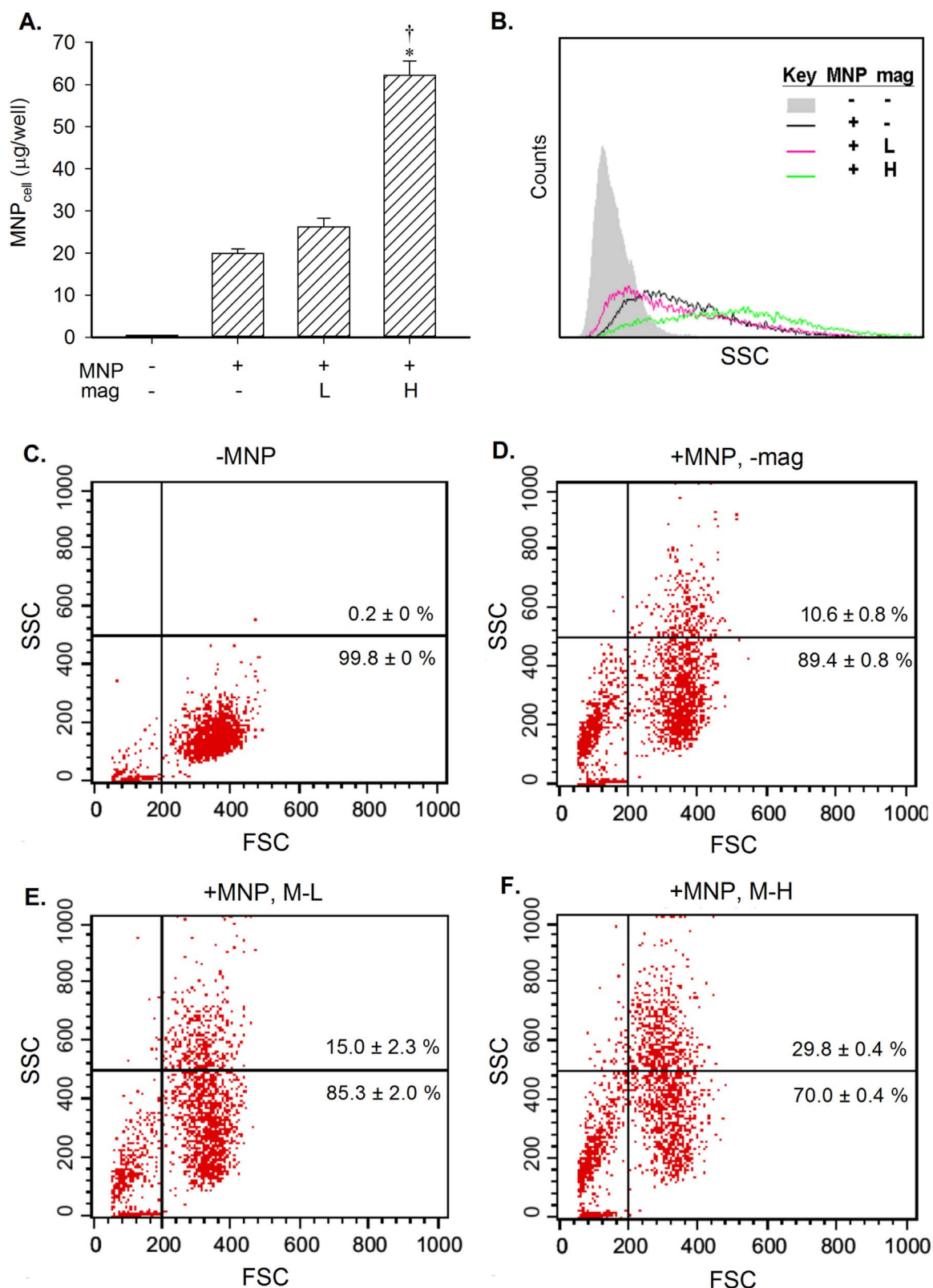


Fig. 3. Inhomogeneous MNP Uptake under Magnetic Field. LN229 cells were incubated with MNP (200 µg/well; 20.8 µg/cm²) for 2 h with magnet of non-uniformed/low (L) or uniformed/high (H) intensity and then immediately processed for iron assay (A) and flow cytometry (B-F). Data shown were mean ± SE. Numbers indicate % cell number of defined area (n=3). *, *p* < 0.05 compared with control group without magnet; †, *p* < 0.05 compared with the L group.

that the MNP_{cell} increased in the presence of the magnet, despite of the arrangement of magnets; whereas the fraction of SSC > 300 in M-L group was approximately 50% of that in other groups. In addition, the cells located in SSC > 600 region was about 3-fold with H-field (M-H or

M-F) vs. L-field (M-L), suggesting the magnet underneath H-wells may significantly increase the MNP_{cell} in a small population of cells in L wells, despite the uniformity variation of the magnetic field. The fraction of FSC > 300 in L-field (M-L) was 1.2-fold of that in H-field

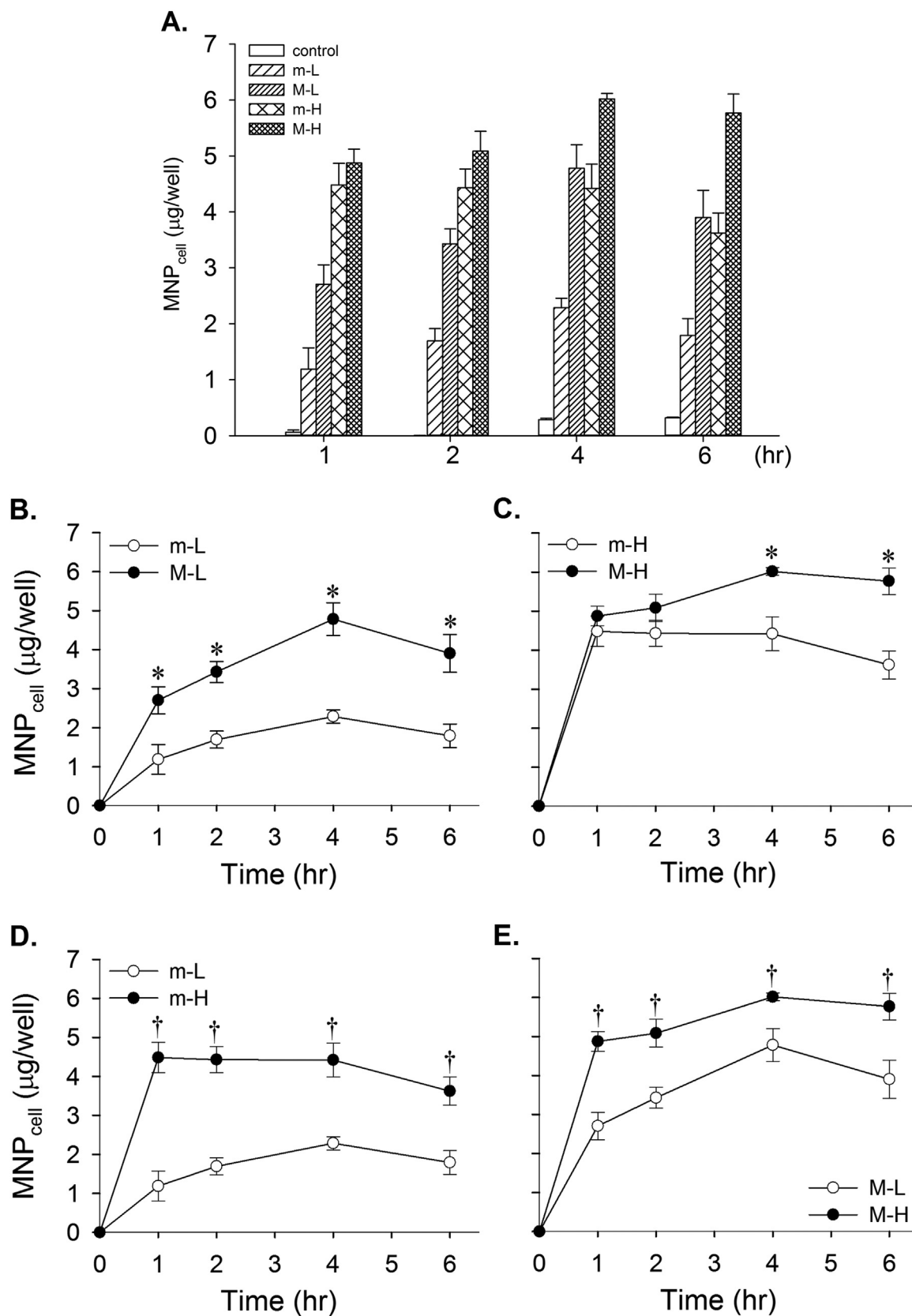


Fig. 4. Time-dependent MNP uptake by LN229 cells. LN229 cells were exposed to MNPs (10 μg/well; 5 μg/cm²) for different time periods with non-uniformed/low (L) or uniformed/high (H) magnet field for one minute (m) or during the incubation time as indicated (M). Data shown were mean ± SE (n=3). *, *p* < 0.05 compared with corresponding m group; †, *p* < 0.05 compared with corresponding L group.

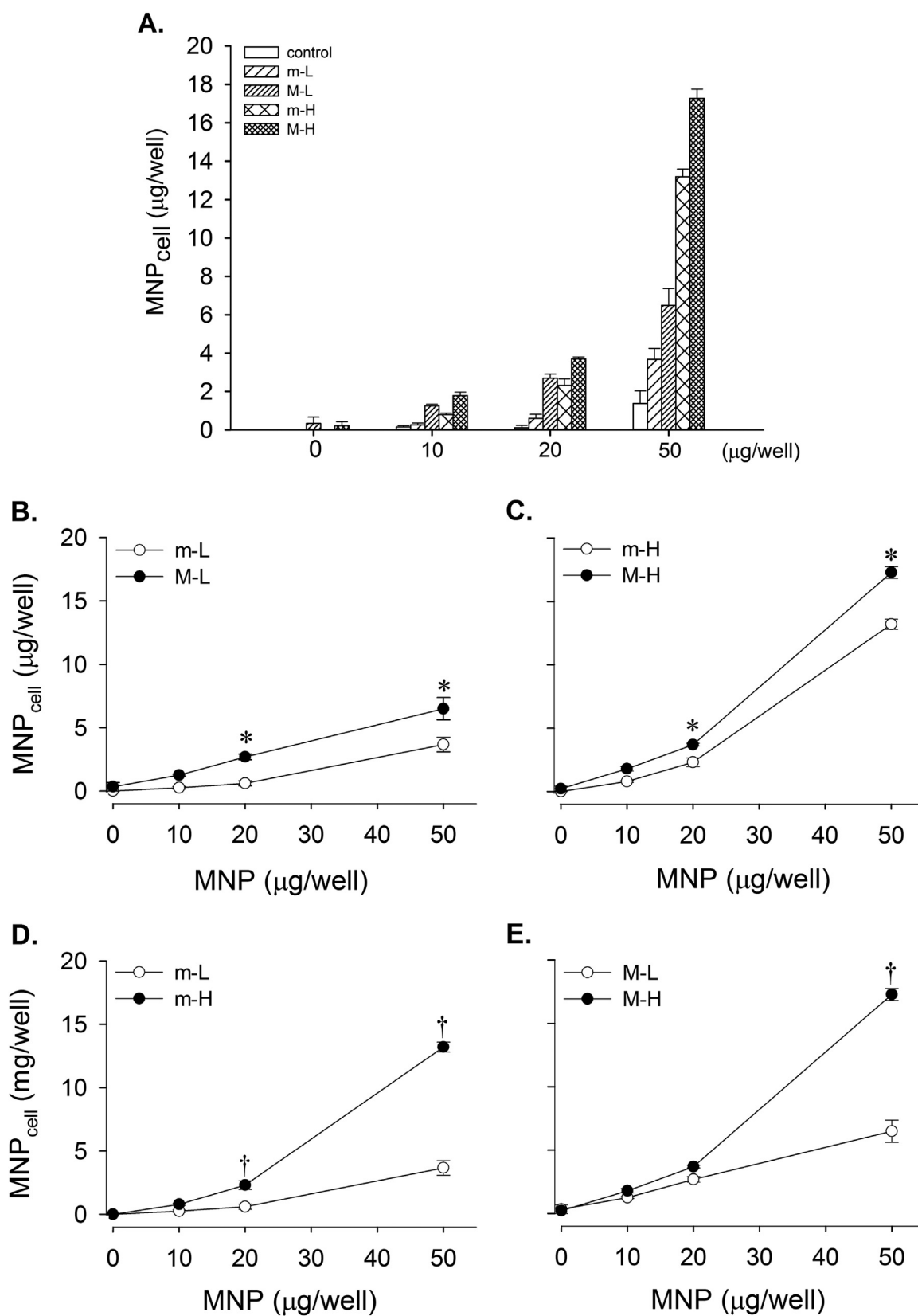


Fig. 5. Concentration-dependent MNP uptake by LN229 cells. LN229 cells were exposed to MNPs (10–50 µg/well; 5–25 µg/cm²) for 2 h with magnet of non-uniformed/low (L) or uniformed/high (H) intensity for one min (m) or during the whole incubation time (M). Data shown were mean ± SE (n=3). *, *p* < 0.05 compared with corresponding m group; †, *p* < 0.05 compared with corresponding L group.

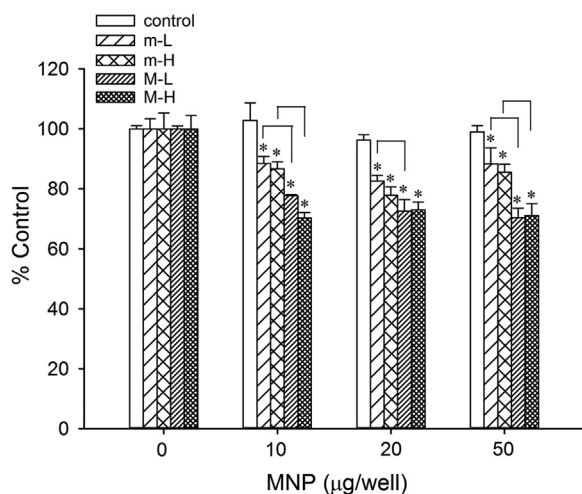


Fig. 6. MNP inhibited mitochondria metabolic activity of LN229 cells in the presence of magnetic field. LN229 cells were exposed to MNPs (10–50 µg/well; 5–25 µg/cm²) for 2 h with non-uniformed/low (L) or uniformed/high (H) magnetic field for one min (m) or during the whole incubation time (M) prior to MTT assay. Data shown were mean ± SE (n=3). *, p < 0.05 compared with cells incubated with the corresponding controls without magnetic field.

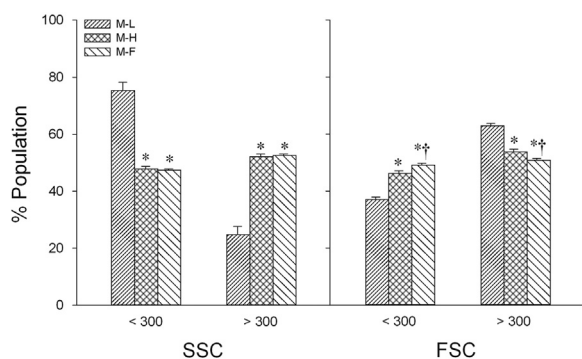


Fig. 7. Magnetic field influenced the cellular complexity and size after MNP uptake. LN229 cells were exposed to MNPs (50 µg/well; 25 µg/cm²) for 2 h with staggered or filled magnet plate underneath followed by the analysis with flow cytometry. Data are presented as mean ± SE (n=5–10). *, p < 0.05 compared with cells in “M-L” field. †, p < 0.05 compared with cells in “M-H” field.

(M-H and M-F), suggesting that the cell size did not increase with MNP uptake.

4. Discussion

The motion of magnetic nanoparticles in an applied magnetic field is governed by several factors including magnetic force, buoyancy, gravity, Brownian dynamics, and magnetic dipole interactions, *etc* [29]. Previous study had demonstrated that magnetic force may dominate particle motion within a height of ~10 mm from the bottom of the well in culture [29]. Magnetic application may provide a driving force that overcome Brownian diffusion to facilitate MNP sedimentation in medium and draw MNPs down in contact with plasma membrane. Therefore, magnetic force may concentrate MNPs on the cellular surface, increase interaction of MNPs with cells, and enhance internalization. Application of magnetic force with staggered plate allows study of MNP internalization by cells subjected to non-uniformed/low (L) or uniformed/high (H) magnetic field. The H-field may facilitate even distribution of MNPs in culture, whereas L-field may simulate magnetic application on tissue/cells *in vivo*. In this study, magnet-induced MNP internalization has been demonstrated with dark field microscopy, flow cytometry and a colorimetric assay for iron content.

Although assessment by these methods only reveals cell associated MNPs, our previous finding suggested that these cells are prone to internalize fluorescent MNPs within 2 h using confocal microscopy [26]. MNPs conjugated with fluorophore are required for confocal microscopy, but such modification may potentially alter surface characteristics of MNPs, and thus alter its interaction with cell membrane, and hence internalization. Therefore, the dark field microscopy may serve as a sensitive method for observation of internalization of label-free MNPs.

Previous studies have demonstrated the use of cylindrical magnets underneath every well in a 96-well plate for magnetofection [9,10,21]. It is anticipated that adjacent magnets may influence each other, resulting in higher magnetic field at the sites proximal to the adjacent wells and difficulty to achieve homogenous distribution of MNPs on the surface of cells in the same well [9,21]. In our study, such magnetic force generated from the magnet underneath adjacent wells created enough of driving force on MNPs in wells without magnet underneath (L-field) in the staggered plate. Therefore, the magnetic plate with staggered arrangement may be used to generate a relatively uniformed field, and thus avoid the influence of neighboring magnets on the magnetic flux density [21]. Nevertheless, there was no significant difference in MNP uptake between H-fields in staggered plate (M-H) and in magnetic plate with magnets underneath every well (M-F), as analyzed by flow cytometry (Fig. 7). Previous study also indicated that 3.8–4.2 kG did not exert difference in MNP uptake by astrocytes [19]. It appears that biological variation may out weight that potentially induced by such variation in magnetic field.

With the relatively high and uniformed magnetic field (H-field; Fig. 4C), continuous application of the magnetic force did not further increase MNP_{cell} from that induced by application of H-field for one min. Therefore, the major effect of the external magnetic field to uptake of PAA-coated MNP within 2 h may be due to magnet-induced MNP sedimentation in the culture medium. The results are consistent with our previous finding with dextran-coated MNP in LN229 cells [26]. Although gravity [36,37] and presumably magnetic force upon nanoparticles, and indirectly plasma membrane, may facilitate endosome formation or internalization [21,28], MNP adsorbed on the cell surface or in the endosome cannot be differentiated in the current study.

In contrast to the H-field, the cells in the L-field were subjected to relatively low and non-uniformed magnetic force up to 33-fold in difference (Table 1). However, averaged MNP_{cell} in L-field was 56–80% of that in the H-field at different time points (Fig. 4E) in spite of very small portion (< 10%; left insert of Fig. 1D) of cells was in contact with most of MNPs due to non-uniformed magnetic flux density in the L-field. The surprisingly high MNP_{cell} in L-field may be due to high uptake capacity of MNPs, as shown in Fig. 5. It has been demonstrated that PAA-coated MNP may also be internalized by human neuroblast [35] and Chinese hamster ovary cells [21]; internalization may reach plateau after incubation without magnet for 8–12 h [34]. Under such conditions, human neuroblast may internalize PAA-MNP up to 20 pg/cell [35]. With one-min magnet application, MNP_{cell} was significant higher in cells subjected to H- vs. L-field, which might be due to incomplete sedimentation of MNPs in subjected to L-field in one min (Fig. 4D). Although mitochondrial enzyme activity appears to be lower in cells subjected to continuous exposure to magnetic field (Fig. 6), MNP_{cell} was still higher compared to cells in one-min magnetic field. Thus, no evidence suggested that enzyme activity of dehydrogenase is associated with MNP_{cell}.

With flow cytometry, MNP induced an increase in SSC and decrease in FSC. Our results are consistent with previous studies demonstrating that increased nanoparticle internalization is associated with an increase in SSC and a decrease in FSC [38], suggesting reduced size of cells. Nanoparticles internalization may alter actin cytoskeleton architecture, microtubule network, and reduce cell size [39,40]. Alternatively, reduced FSC may be partly due to reduced amount of light reaching the forward scatter detector by absorption or reflection

of light by the particles [38,41].

Although increased SSC was observed with MNP administration and application of magnetic field, variation of SSC distribution suggested variation of MNP internalization in cell population studied. Recent studies have demonstrated that nanoparticle internalization may differ between cell cycle phases [42,43], with the highest nanoparticle uptake in the G2/M phase and lowest in G0/G1 phase. Therefore, subpopulations of cells in different cell cycle phases may be responsible for the diversity in MNP_{cell} observed in our study. Nevertheless, similar effects were observed in cells cultured in the H-field of both plates. Therefore, MNP internalization in H-field of staggered plate cannot be differentiated from that of the filled magnet plate due to biological variation.

Manipulation of magnetic field *in vitro* may serve as a model system for application of magnetic field *in vivo* to achieve target delivery of genes/drugs. It is well known that the abnormal blood vessels that synthesized by tumor-induced angiogenesis exert large pores ranging between 380 and 780 nm in diameter [44,45], allowing nanoparticles to reach the perivascular space and accumulate in the tumor interstitium *via* enhanced permeability and retention effect [45]. Recent studies have demonstrated that under the influence of an external magnetic force, MNP may serve as a promising platform to deliver therapeutic cargos to targeted site such as solid tumor or brain [46–48]. It is anticipated that magnetic targeting allows MNP retention in the vessels around the tumor, and subsequently tumor interstitial, the inhomogeneous uptake in the tumor is expected. Controlling drug release in the extracellular space may ensure more exposure of tumor cells to the drugs, and thus better therapeutic effect. Our results suggested that magnetic field may enhance overall MNP uptake to a similar degree regardless of the uniformity of magnetic field.

5. Conclusion

Our study suggests that enhanced sedimentation may be the major mechanism underlies the effects of magnetic force on MNP internalization; spatial separation of the magnets under the cultured cells may be considered if biological variation was reduced, such as in synchronized cells. The finding supports utilization of all wells on the culture plate in study of magnetic influence on cultured cells to reduce cost and increase efficiency in such experiments.

Acknowledgement

This work was supported by grants from Ministry of Science and Technology, Taiwan (NSC 100–2120-M-182-001-), National Health Research Institute, Taiwan (NHRI-EX9909937E1), Healthy Aging Research Program at Chang Gung University (EMRPD1E1651), and Chang Gung Memorial Hospital (BMRP432). The authors thank Dr. Shieh-Yueh Yang and Dr. Hsin-Hsien Chen at MagQu Co., Ltd. for magnetic field measurement.

References

- N. Lewinski, V. Colvin, R. Drezek, Cytotoxicity of nanoparticles, *Small* 4 (2008) 26–49.
- O. Veisoh, J.W. Gunn, M. Zhang, Design and fabrication of magnetic nanoparticles for targeted drug delivery and imaging, *Adv. Drug Deliv. Rev.* 62 (2010) 284–304.
- M. Namdeo, et al., Magnetic nanoparticles for drug delivery applications, *J. Nanosci. Nanotechnol.* 8 (2008) 3247–3271.
- E. Duguet, S. Vasseur, S. Mornet, J.M. Devoisselle, Magnetic nanoparticles and their applications in medicine, *Nanomed. (Lond.)* 1 (2006) 157–168.
- A.K. Gupta, M. Gupta, Synthesis and surface engineering of iron oxide nanoparticles for biomedical applications, *Biomaterials* 26 (2005) 3995–4021.
- U. Schillinger, et al., Advances in magnetofection—magnetically guided nucleic acid delivery, *J. Magn. Magn. Mater.* 293 (2005) 501–508.
- J. Dobson, Gene therapy progress and prospects: magnetic nanoparticle-based Gene delivery, *Gene Ther.* 13 (2006) 283–287.
- C. Plank, O. Zelphati, O. Mykhaylyk, Magnetically enhanced nucleic acid delivery. Ten years of magnetofection—Progress and prospects, *Adv. Drug Deliv. Rev.* 63 (2011) 1300–1331.
- C. Plank, et al., The magnetofection method: Using magnetic force to enhance gene delivery, *Biol. Chem.* 384 (2003) 737–747.
- F. Scherer, et al., Magnetofection: enhancing and targeting gene delivery by magnetic force *in vitro* and *in vivo*, *Gene Ther.* 9 (2002) 102–109.
- B. Thiesen, A. Jordan, Clinical applications of magnetic nanoparticles for hyperthermia, *Int. J. Hyperth.* 24 (2008) 467–474.
- V.I. Shubayev, T.R. Pisanic 2nd, S. Jin, Magnetic nanoparticles for theragnostics, *Adv. Drug Deliv. Rev.* 61 (2009) 467–477.
- C. Sun, J.S. Lee, M. Zhang, Magnetic nanoparticles in MR imaging and drug delivery, *Adv. Drug Deliv. Rev.* 60 (2008) 1252–1265.
- C. Corot, P. Robert, J.M. Idee, M. Port, Recent advances in iron oxide nanocrystal technology for medical imaging, *Adv. Drug Deliv. Rev.* 58 (2006) 1471–1504.
- Wahajuddin, S. Arora, Superparamagnetic iron oxide nanoparticles: magnetic nanopatforms as drug carriers, *Int. J. Nanomed.* 7 (2012) 3445–3471.
- T. De Jardin, et al., Influence of both a static magnetic field and penetratin on magnetic nanoparticle delivery into fibroblasts, *Nanomed. (Lond.)* 6 (2011) 1719–1731.
- C. Dahmani, et al., Rotational magnetic pulses enhance the magnetofection efficiency *in vitro* in adherent and suspension cells, *J. Magn. Magn. Mater.* 332 (2013) 163–171.
- C. MacDonald, K. Barbee, B. Polyak, Force dependent internalization of magnetic nanoparticles results in highly loaded endothelial cells for use as potential therapy delivery vectors, *Pharm. Res.* 29 (2012) 1270–1281.
- M.C. Lamkowsky, M. Geppert, M.M. Schmidt, R. Dringen, Magnetic field-induced acceleration of the accumulation of magnetic iron oxide nanoparticles by cultured brain astrocytes, *J. Biomed. Mater. Res. Part A* 100 (2012) 323–334.
- Q. Liu, J. Zhang, W. Xia, H. Gu, Magnetic field enhanced cell uptake efficiency of magnetic silica mesoporous nanoparticles, *Nanoscale* 4 (2012) 3415–3421.
- S. Prijic, et al., Increased cellular uptake of biocompatible superparamagnetic iron oxide nanoparticles into malignant cells by an external magnetic field, *J. Membr. Biol.* 236 (2010) 167–179.
- I. Canton, G. Battaglia, Endocytosis at the nanoscale, *Chem. Soc. Rev.* 41 (2012) 2718–2739.
- F. Zhao, et al., Cellular uptake, intracellular trafficking, and cytotoxicity of nanomaterials, *Small* 7 (2011) 1322–1337.
- S. Mishra, P. Webster, M.E. Davis, PEGylation significantly affects cellular uptake and intracellular trafficking of non-viral gene delivery particles, *Eur. J. Cell Biol.* 83 (2004) 97–111.
- B. Pelaz, et al., Surface functionalization of nanoparticles with polyethylene glycol: effects on protein adsorption and cellular uptake, *ACS Nano* 9 (2015) 6996–7008.
- Y.C. Lu, et al., Augmented cellular uptake of nanoparticles using tea catechins: effect of surface modification on nanoparticle-cell interaction, *Nanoscale* 6 (2014) 10297–10306.
- D. Fayol, N. Luciani, L. Lartigue, F. Gazeau, C. Wilhelm, Managing magnetic nanoparticle aggregation and cellular uptake: a precondition for efficient stem-cell differentiation and MRI tracking, *Adv. Healthc. Mater.* 2 (2013) 313–325.
- C.A. Smith, et al., The effect of static magnetic fields and tat peptides on cellular and nuclear uptake of magnetic nanoparticles, *Biomaterials* 31 (2010) 4392–4400.
- E.P. Furlani, X. Xue, Field, force and transport analysis for magnetic particle-based gene delivery, *Microfluid. Nanofluidics* 13 (2012) 589–602.
- Y.H. Ma, et al., Magnetically targeted thrombolysis with recombinant tissue plasminogen activator bound to polyacrylic acid-coated nanoparticles, *Biomaterials* 30 (2009) 3343–3351.
- V.B.B. Mojca Pavlin, Stability of nanoparticle suspensions in different biologically relevant media, *Dig. J. Nanomater. Biostruct.* 7 (2012) 1389–1400.
- C.L. Lin, C.F. Lee, W.Y. Chiu, Preparation and properties of poly(acrylic acid) oligomer stabilized superparamagnetic ferrofluid, *J. Colloid Interface Sci.* 291 (2005) 411–420.
- V.B. Bregar, J. Lojk, V. Šuštar, P. Veranic, M. Pavlin, Visualization of internalization of functionalized cobalt ferrite nanoparticles and their intracellular fate, *Int. J. Nanomed.* 8 (2013) 919–931.
- J. Lojk, et al., Cell type-specific response to high intracellular loading of polyacrylic acid-coated magnetic nanoparticles, *Int. J. Nanomed.* 10 (2015) 1449–1462.
- M.P. Calatayud, et al., The effect of surface charge of functionalized Fe_3O_4 nanoparticles on protein adsorption and cell uptake, *Biomaterials* 35 (2014) 6389–6399.
- E.C. Cho, Q. Zhang, Y. Xia, The effect of sedimentation and diffusion on cellular uptake of gold nanoparticles, *Nat. Nanotechnol.* 6 (2011) 385–391.
- T. Zhu, Z. Jiang, Y. Ma, Adsorption of nanoparticles and nanoparticle aggregates on membrane under gravity, *Appl. Phys. Lett.* 102 (2013) 153109.
- R.M. Zucker, E.J. Massaro, K.M. Sanders, L.L. Degen, W.K. Boyes, Detection of TiO_2 nanoparticles in cells by flow cytometry, *Cytom. A* 77A (2010) 677–685.
- S.J.H. Soenen, N. Nuytten, S.F. De Meyer, S.C. De Smedt, M. De Cuyper, High intracellular iron oxide nanoparticle concentrations affect cellular cytoskeleton and focal adhesion kinase-mediated signaling, *Small* 6 (2010) 832–842.
- S.J.H. Soenen, et al., The role of nanoparticle concentration-dependent induction of cellular stress in the internalization of non-toxic cationic magnetoliposomes, *Biomaterials* 30 (2009) 6803–6813.
- A. Kumar, A.K. Pandey, S.S. Singh, R. Shanker, A. Dhawan, A flow cytometric method to assess nanoparticle uptake in bacteria, *Cytom. A* 79A (2011) 707–712.
- A.H. Abouzeid, V.P. Torchilin, The role of cell cycle in the efficiency and activity of cancer nanomedicines, *Expert Opin. Drug Deliv.* 10 (2013) 775–786.
- J.A. Kim, C. Aberg, A. Salvati, K.A. Dawson, Role of cell cycle on the cellular uptake

- and dilution of nanoparticles in a cell population, *Nat. Nano* 7 (2012) 62–68.
- [44] I. Brigger, C. Dubernet, P. Couvreur, Nanoparticles in cancer therapy and diagnosis, *Adv. Drug Deliv. Rev.* 54 (2002) 631–651.
- [45] N. Bertrand, J. Wu, X. Xu, N. Kamaly, O.C. Farokhzad, Cancer nanotechnology: the impact of passive and active targeting in the era of modern cancer biology, *Adv. Drug Deliv. Rev.* 66 (2014) 2–25.
- [46] D. Singh, McMillan, M. JoEllyn, A.V. Kabanov, M. Sokolsky-Papkov, H.E. Gendelman, Bench-to bedside translation of magnetic nanoparticles, *Nanomed. (Lond.)* 9 (2014) 501–516.
- [47] M.S. Muthu, D.T. Leong, L. Mei, S.S. Feng, Nanotheranostics - application and further development of nanomedicine strategies for advanced theranostics, *Theranostics* 4 (2014) 660–677.
- [48] L.S. del Burgo, R.M. Hernandez, G. Orive, J.L. Pedraz, Nanotherapeutic approaches for brain cancer management, *Nanomedicine* 10 (2014) 905–919.